Catal Lett (2016) 146:951–959
DOI 10.1007/s10562-016-1718-5

Magnetic $CoFe_2O_4$ Nanoparticles Supported Basic Poly(Ionic Liquid)s Catalysts: Preparation and Catalytic Performance Comparison in Transesterification and Knoevenagel Condensation

Hong Yuan[1] · Qingze Jiao[1,2] · Yaping Zhang[1] · Jing Zhang[1] · Qin Wu[1] · Yun Zhao[1] · Sneha Neerunjun[1] · Hansheng Li[1]

Received: 17 January 2016 / Accepted: 21 February 2016 / Published online: 29 February 2016

Abstract Magnetic $CoFe_2O_4$ nanoparticles supported basic poly(ionic liquid)s catalysts were successfully synthesized, and the catalysts prepared through the surface grafting method showed a higher loading amount of ionic liquids, better stability and excellent paramagnetism than that prepared by the conventional co-polymerization method. The catalytic activities for the transesterification and for the Knoevenagel condensation were evaluated, and the catalysts showed an excellent catalytic performance as opposed to the sample prepared using the copolymerization method. The yields of the objective products in transesterification and Knoevenagel condensation were 93 and 97 %, respectively. Moreover, the catalysts could be easily recovered with the assistance of an external magnetic field and after being reused four times, they retained about 76.1 and 68.5 % of their catalytic performance, respectively.

Graphical Abstract

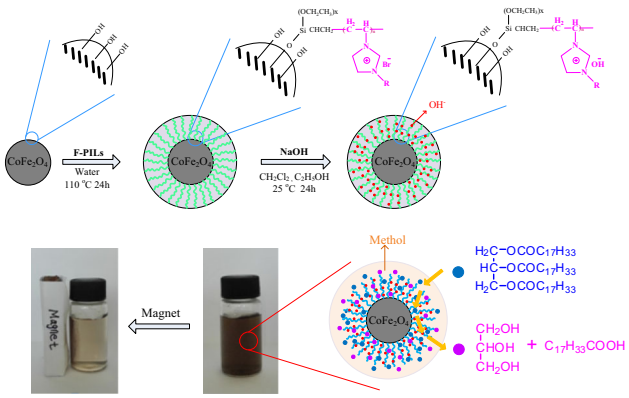

Keywords Magnetic $CoFe_2O_4$ nanoparticles · Supported catalysts · Basic poly(ionic liquid)s · Transesterification · Knoevenagel condensation

1 Introduction

Ionic liquids (ILs) have shown a promising interest in catalytic fields due to the following properties namely non-volatility, wide temperature range of liquid state, high thermal stability, excellent solubility of organic and inorganic materials and tenability of structures [1–3]. However, the good solubility of ILs in the reaction system makes the recovery of the homogeneous catalysts difficult and limits their widespread application. Poly (IL)s or polymerized ionic liquids (PILs), which carry IL species in each repeating unit, become a new way of processing in the field of polymer chemistry, catalysis and materials science [4]. In the catalytic field, PILs have been the most preferred

✉ Hansheng Li
hanshengli@bit.edu.cn

[1] School of Chemical Engineering and the Environment, Beijing Institute of Technology, Beijing 100081, China

[2] School of Chemical Engineering and Materials Science, Beijing Institute of Technology, Zhuhai, Zhuhai 519085, China

choice due to their high active sites and excellent recovery as they combine the advantages of both ILs with homogeneous catalysis and polymers with high catalytic activities [5–7]. Therefore, the PILs catalysts have been widely used in cycloaddition [8], oxidative carbonylation [9], hydrogenation reaction [10], Heck arylation [11], and aldolization [12, 13]. However, the use of the PILs as homogeneous catalysts leads to the difficulties in separation and recovery of the catalysts from the reaction mixture via traditional separation methods such as filtration, free sedimentation and centrifugation, which greatly restricts their widespread utilization in industry.

Magnetic nanoparticles (MNPs) work on the basis of magnetic properties, thus the MNPs can be easily collected in a magnetic field. This feature of MNPs has been appreciated by researchers and successfully used to support catalysts [14–23]. In order to resolve the drawbacks of difficult separation for ILs as homogeneous catalysts, an effective approach is to support ILs on MNPs. Moreover, these supported catalysts can be not only designed and tuned, but also recycled rapidly in a magnetic field [14–16]. However, the major problem with using MNPs supported ILs catalysts is low loading catalytic active species onto the surface of MNPs. Hence, in the catalytic reaction systems, the catalysts with high active sites are needed under the same catalysts loading.

Moreover, because the PILs exhibited more activity sites, MNPs supported PILs catalysts have received more attention in recent years [17, 18]. At present, there are two main methods for preparation of supported PILs, as surface initiated radical copolymerization method and surface grafting poly (IL)s approach, respectively. Generally, functionalized poly (IL)s catalysts coated on MNPs were prepared by using the radical copolymerization of modified MNPs with ILs monomers and were reported to possess high activities, recoverability and easy separability [19–21]. Therefore, MNPs supported poly (IL)s catalysts have been widely used in catalytic reactions, due to their higher surface area, better recycling capability and catalytic performance. However, to the best of our knowledge, there are few works to identify advantages and disadvantages of catalysts prepared using the two methods, radical copolymerization method and surface grafting. In this case, the catalytic performance of catalysts prepared by radical copolymerization and surface grafting were systematically investigated and compared.

In this present work, two methods to prepare the magnetic $CoFe_2O_4$ nanoparticle (MCF) supported basic poly (IL)s catalysts (PILs/MCFs) were proposed and their catalytic activities for the transesterification and the Knoevenagel condensation were compared.

2 Experimental

2.1 Materials and Methods

$CoCl_2{\cdot}6H_2O$, $Fe(NO_3)_3{\cdot}9H_2O$, Triton X-100, n-hexane, n-hexanol, methylamine solution, tetraethoxysilane (TEOS), alkyl bromides (Alkyl = n-propyl, n-hexane, or n-dodecyl), benzaldehyde, ethyl cyanoacetate and glycerol trioleate (TG) were purchased from Sinopharm Chemical Reagent Co., Ltd (Beijing, China). 3-Vinyl-triethoxysilane was purchased from Acros Organics (Geel, Belgium). 1-Vinyl imidazole was purchased from J&K scientific Co., Ltd (Beijing China). Acetonitrile, methanol, alcohol, diethyl ether, acetone, azodiisobutyronitrile (AIBN), N,N-dimethylformamide (DMF),dichloromethane and NaOH were obtained from Beijing Chemical Works (Beijing, China). AIBN was purified before use.

2.2 Preparation of MCFs and IL

MCFs were achieved by alkali-treating $CoFe_2O_4/SiO_2$, which was prepared through the sol–gel process mediated in an inverse micro-emulsion, referring to the previous works of our group [24, 25].

IL monomers [VRIm][Br] (R = n-propyl, n-hexane, n-dodecyl) were synthesized by the quarterisation reaction between 1-vinyl imidazole and alkyl bromide. The typical process for preparing IL is as follows: 1-vinyl imidazole and alkyl bromides (Alkyl = n-propyl, n-hexane, or n-dodecyl) were added into the flask with methanol as solvent and then reacted at 60 °C for 24 h. After being washed with diethyl ether and dried at 45 °C successively, the IL monomers [VPIm][Br], [VHIm][Br] and [VDoIm][Br] were obtained.

2.3 Preparation of Catalysts

2.3.1 Preparation Using a Co-Polymerization Method (co-PILs/MCFs)

The co-PILs/MCFs catalysts were prepared through the copolymerization between vinyl imidazole ILs and vinyl functionalized MCFs (V-MCFs) as shown in Scheme 1. Firstly, 1.0 mmol of 3-vinyl-triethoxysilane was added into the solution containing 1.403 g of MCFs and reacted at 110 °C for 24 h. After being washed with acetone, the black V-MCFs were obtained. Secondly, 0.02 mol of [VRIm][Br] and 1.5928 g (containing about 1 mmol of vinyl) of V-MCFs were added into a hydrothermal reactor and copolymerized at 60 °C for 24 h, with acetonitrile as solvent and 1.0 mmol of AIBN as initiator, after being

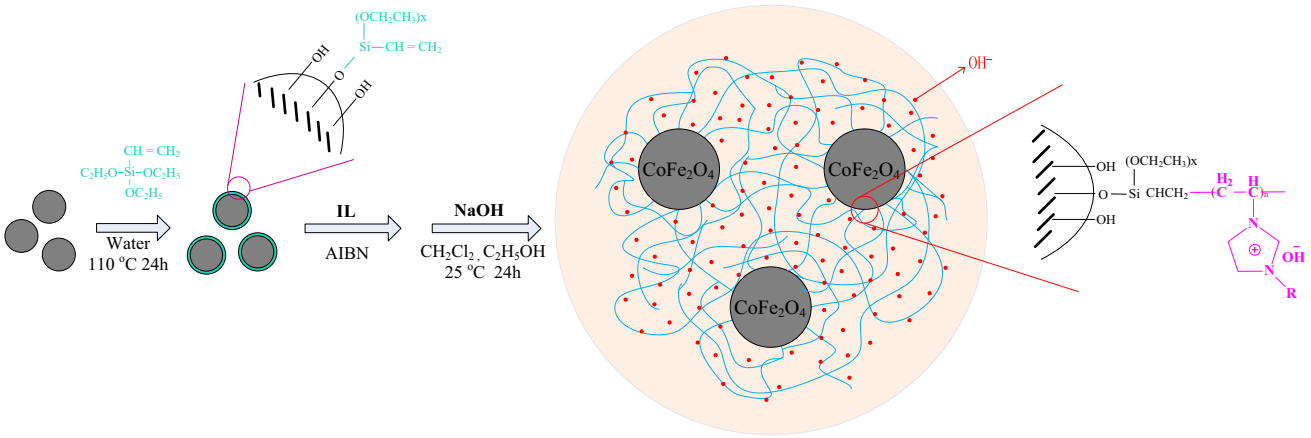

Scheme 1 The procedure for preparation of co-p[VRIm][OH]/MCFs

washed with methanol and dried in vacuum oven, thus the MCFs supported PILs were obtained. According to the length of alkyl chains (R), the supported poly(IL)s were denoted as co-p[VRIm][Br]/MCFs (R = propyl, hexyl or dodecyl). Finally, co-p[VRIm][Br]/MCFs, dichloromethane, NaOH were added into the flask and reacted for 24 h at room temperature, the MCFs supported basic PILs were achieved after being dried at 55 °C, denoted as co-p[VRIm][OH]/MCFs.

2.3.2 *Preparation Using the Surface Grafting Method (g-PILs/MCFs)*

The preparation of g-PILs/MCFs catalysts through the surface grafting method was shown in Scheme 2. Firstly, 0.02 mol of [VRIm][Br] and 1.0 mmol of 3-vinyl-triethoxysilane were added into the flask with DMF as solvent, and the polymerization were carried out under nitrogen atmosphere with 1.0 mmol of AIBN as initiator at 60 °C for 24 h, to obtain the triethoxysilane functionalized poly(IL)s (F-PILs). Then, 1.403 g of MCFs were added and transferred into a hydrothermal reactor and reacted at 110 °C for 24 h. After being washed with methanol and dried in vacuum oven at 50 °C, the g-PILs/MCFs were obtained. According to the length of alkyl chains (R), the g-PILs/MCFs were denoted as g-p[VRIm][Br]/MCFs (R = propyl, hexyl or dodecyl). Finally, g-p[VRIm][Br]/MCFs, dichloromethane, alcohol and NaOH were added into the flask and reacted for 24 h at room temperature. The MCFs supported basic PILs were achieved after drying at 55 °C and was denoted as g-p[VRIm][OH]/MCFs.

2.4 Catalysts Characterization

Fourier transform infrared spectrometry (FTIR) analysis was conducted by using Nicolet iS10 Fourier transform infrared spectrometer (Thermo scientific, America) in a frequency range of 4000–450 cm^{-1} with a solution of 4 cm^{-1}, a scanning number of 16 and KBr as a reference. Elemental analysis of the solids (C, H, N concentrations) was obtained using a Vario ELV5.19.6 organic element analyser (Elemental Analyser system GmbH, Germany).

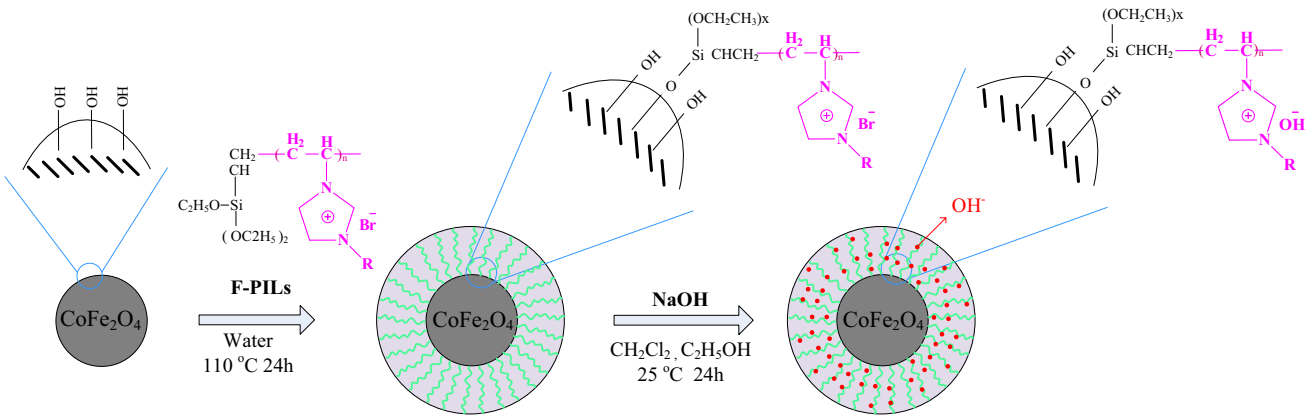

Scheme 2 The procedure for preparation of g-p[VRIm][OH]/MCFs

Thermo gravimetric and differential thermal analysis (TG/DTA) was carried out on a TG/DTA 6200 (SII Nano Technology Inc., Japan), by heating the samples under N_2 atmosphere from room temperature to 700 °C at a heating rate of 10 K/min. X-ray powder diffraction (XRD) analysis of samples was collected by an Ultima IV X-ray diffractometer (Rigaku, Japan) with CuKα radiation. Transmission electron microscopy (TEM) was performed with a JEM-2100 transmission electron microscope (JEOL, Japan) to observe the microstructure of the samples. Magnetism analysis was carried out on a JLDJ 9600 vibrating sample magnetometer (LD, America).

2.5 Catalytic Performances Evaluation

The catalytic activities were evaluated using the transesterification of TG with methanol and the Knoevenagel condensation of benzaldehyde and ethyl cyanoacetate. The amounts of the catalysts were 1 wt.% of TG used in the transesterification and 1 wt.% of benzaldehyde used in the Knoevenagel reaction, respectively.

2.5.1 Transesterification Reaction

The transesterification reaction process was schematically depicted in Scheme 3. Firstly, TG was reacted with methanol to produce glyceryl dioleate (denoted as DG) and methyl oleate (ME), whereby the intermediate product DG was further reacted with methanol to further yield glyceryl monooleate (MG) and ME. In the end, glycerin and ME were produced by the reaction between MG and methanol. Therefore, the yields of ME, DG, MG were used to evaluate the catalytic performance of catalysts.

A 500 mmol methanol, 1.95 mmol TG, the co-p[VRIm][OH]/MCFs or g-p[VRIm][OH]/MCFs catalyst were added into a 40 mL hydrothermal reactor and were reacted at 170 °C for 6 h. After the reaction was completed, the catalyst was separated by the external magnetic field for recycling. The components were determined by liquid chromatography (HPLC, Techcomp LC2000) equipped with an ultraviolet photo-metric detector ($\gamma = 210$ nm). A Kromasil 100-5C18 column (4.6 mm × 5 μm × 250 mm) was used for testing and the column temperature was maintained at 25 °C. The mobile phase consisted of a mixture of acetonitrile and acetone (1:1 in volumetric ratio) at a flow rate of 1.0 ml/min. The yield of ME (Y_{ME}) and the selectivities of products (S_i, i = DG, MG, ME) were calculated according to the equations listed below.

$$Y_{ME} = \frac{n_{ME}}{3 \times n_{TG,0}},\ S_i = \frac{i \times n_i}{\sum_{j=1}^{3} j \times n_j} \times 100\ \%$$

2.5.2 Knoevenagel Condensation

The Knoevenagel condensation between benzaldehyde and ethyl cyanoacetate is irreversible, as such the catalytic performance of catalysts could be evaluated by the conversion of benzaldehyde. A 0.01 mol benzaldehyde, 0.01 mol ethyl cyanoacetate, 2 ml methanol and co-p[VRIm][OH]/MCFs or g-p[VRIm][OH]/MCFs catalysts were added into the flask and reacted at 60 °C. After the completion of the reaction, the samples were analyzed by liquid chromatography equipped with an ultraviolet photometric detector ($\gamma = 254$ nm). A Kromat C18 reversed phase silica gel column was used for testing and the column temperature was maintained at 25 °C. The mobile phase consisted of a mixture of methanol and deionized water (9:1 in volumetric ratio) at a flow rate of 0.3 ml/min.

3 Results and Discussion

3.1 Characterization of Catalysts

The chemical structure of co-p[VDoIm][OH]/MCFs and g-p[VDoIm][OH]/MCFs were characterized by FT-IR as shown in Fig. 1. In the FTIR spectrum, the absorption peaks at 806, 1063 cm^{-1} are attributed to M–O vibration (M=Fe or Co) and antisymmetric and symmetric O–Si–O stretching vibrations, respectively [26]. Furthermore, The presence of the supported imidazole ILs on the surface of MCFs was confirmed by some characteristic peaks at 1569, 1648, 2855 and 2925 cm^{-1}, which were attributed to the C=N and C=C stretching vibration of imidazole ring, antisymmetric stretching and symmetric stretching of saturated C–H bond, respectively [27, 28]. The result indicated that the PILs were successfully supported on the

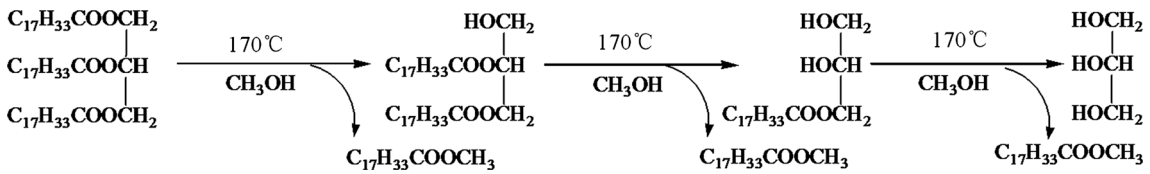

Scheme 3 The process of transesterification of TG with methanol

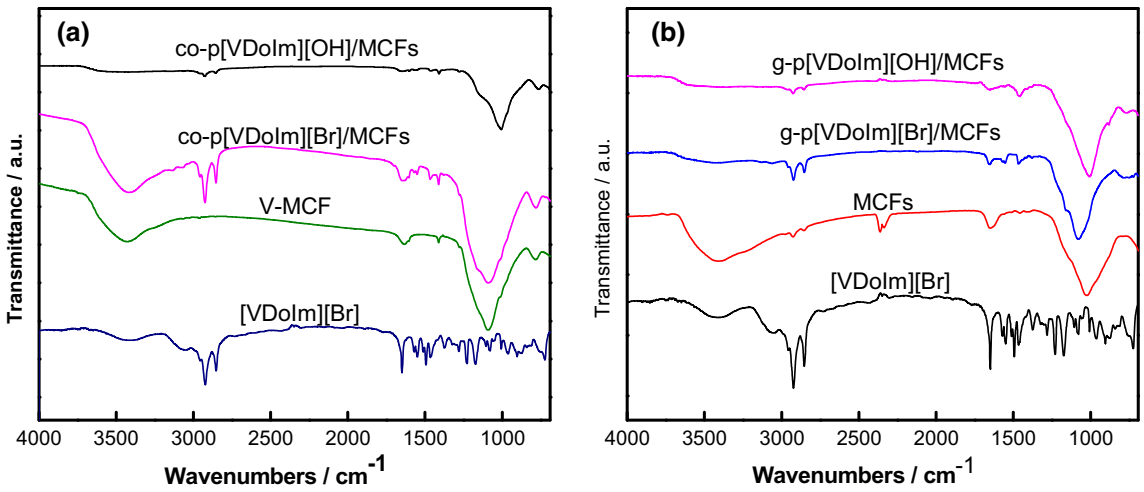

Fig. 1 FTIR spectra of supported PILs **a** co-p[VDoIm][OH]/MCFs **b** g-p[VDoIm][OH]/MCFs

surface of MCFs. The morphology and crystal structure of PILs/MCFs were characterized by TEM and XRD as shown in Figs. 2 and 3 respectively. It can be seen from Fig. 2 that the nano-structure MCFs (black particles) with an average size of 19–21 nm were dispersed in the poly (ILs) (light gray structure) after the loading process. Moreover, in co-p[VDoIm][OH]/MCFs, MCFs were aggregated and coated by PILs as shown in Fig. 2a, while MCFs were well dispersed in g-p[VDoIm][OH]/MCFs. This may be due to the radical copolymerization which resulted in the cross-linking of the polymer matrix. The XRD patterns of co-p[VDoIm][OH]/MCFs and g-p[VDoIm][OH]/MCFs were similar to the diffraction peaks of $CoFe_2O_4$ (JCPDS PDF#22-1086), which means that the structure of MCFs was not destroyed during the loading process and the ion-exchange process.

The PILs/MCFs presented excellent paramagnetism as listed in Table 1, because of the existence of cobalt ferrite. The saturation magnetization (Ms) and remnant magnetization (Mr) of g-p[VDoIm][OH]/MCFs are 13.10 and 0.04 emu/g, and the corresponding data for co-p[VDoIm][OH]/MCFs are 7.76 and 0.09 emu/g, respectively. Thus, the high magnetic responsivity and paramagnetism allowed the catalysts to be separated from the reaction

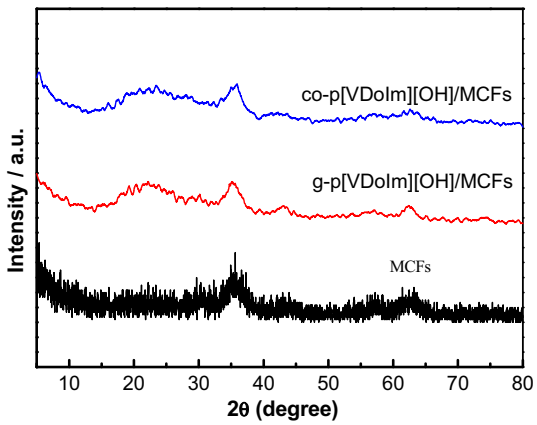

Fig. 3 XRD patterns of supported poly(ionic liquid)s catalysts

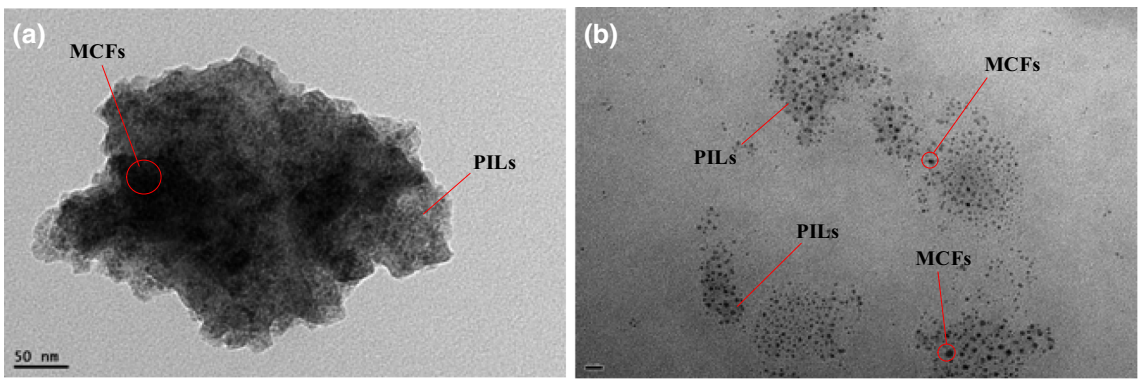

Fig. 2 TEM images of supported poly(ionic liquid)s catalysts. **a** co-p[VRIm][OH]/MCFs and **b** g-p[VRIm][OH]/MCFs

Table 1 Magnetization data of co-p[VDoIm][OH]/MCFs and g-p[VDoIm][OH]/MCFs

Samples	M_s (emu/g)	M_r (emu/g)	Coercivity (G)
co-p[VDoIm][OH]/MCFs	7.76	0.09	66.20
g-p[VDoIm][OH]/MCFs	13.10	0.04	9.37

Fig. 4 Magnetic separation of PILs/MCFs

system rapidly under the effect of the magnetic field, as shown in Fig. 4.

To further determine the loading amount of the catalysts, the elemental analysis (Table 2) and thermogravimetry (TG) analysis (Fig. 5) were carried out. The results of elemental analysis revealed that there are 2.4674 and 3.4057 % of N element for co-p[VDoIm][OH]/MCFs and g-p[VDoIm][OH]/MCFs, which is equal to an PILs loading of 0.8809 and 1.2162 mmol/g respectively. Therefore, it can be concluded that the PILs were successfully bonded onto the surface of MCFs.

The thermal stability of PILs/MCFs was investigated by TG analysis. The TG curves showed that the degradation temperatures of co-p[VDoIm][OH]/MCFs and g-p[VDoIm][OH]/MCFs were about 220 °C. In addition, the weight loss percentages of co-p[VDoIm][OH]/MCFs were about 25 %, whereas the weight loss percentages of g-p[VDoIm][OH]/MCFs were about 35 %. According to the results, it can be deduced that the loading of g-p[VDoIm][OH]/MCFs was 1.2480 mmol/g, which is generally higher than 0.8914 mmol/g for co-p[VDoIm][OH]/MCFs. The loading of PILs obtained from TG analysis was found to be in good agreement with elemental analysis.

In order to compare the alkalinity of the two types of catalysts, acid–base titration analysis was employed for the different types of catalysts with the same quantity [29]. It was found that the catalyst prepared by surface grafting had a higher alkalinity than the catalyst prepared by the copolymerization. The concentration of OH^- of the catalyst obtained by grafting is 0.7433 mmol/g, while the concentration of OH^- of the catalyst prepared by radical copolymerization was 0.6481 mmol/g. This may be because the catalyst obtained by grafting has a higher loading. The results were in accordance with TG and elemental analysis.

3.2 Catalytic Performance Evaluation

The catalytic performance of co-p[VRIm][OH]/MCFs and g-p[VRIm][OH]/MCFs were evaluated by using the catalytic transesterification of TG with methanol and the Knoevenagel condensation of benzaldehyde with ethyl cyanoacetate respectively.

3.2.1 Catalytic Performance for Transesterification

Figure 6 displayed the catalytic performances of co-p[VDoIm][OH]/MCFs and g-p[VDoIm][OH]/MCFs catalysts for transesterification reaction. The better performance was observed for g-p[VDoIm][OH]/MCFs catalysts compared to that for co-p[VDoIm][OH]/MCFs. This may be resulted from the combined effect of steric hindrance and active sites. On one hand, the polymerization reaction for g-p[VDoIm][OH]/MCFs occured earlier than the reaction between silicate ester with hydroxyl groups on the surface of MCFs during the preparation of catalysts. As such, the polymers existed on the surface of MCFs and there was few cross-linking among these polymers, it seemed like a brush loading on the surface of MCFs as shown in Fig. 7a. This particular brush-like structure allowed the reactants to diffuse easily into the polymer to come in contact with the active sites and enhanced the catalytic reaction. On the other hand, since there were lots of unsaturated bonds on the surface of MCFs during the preparation of co-p[VDoIm][OH]/MCFs, which resulted in the formation of 3D polymer networks on the surface of the MCFs. This increased the internal diffusion resistance during the catalytic reaction process. The deductive results were in accordance with data of TEM (Fig. 2a). Therefore, this allows the catalytic reaction to occur only on the surfaces of the catalysts (as shown in Fig. 7b). In addition, the catalysts prepared through the grafted polymerization method were possessed of larger loading amount and higher basicity, and provided more active sites on the surface of MCFs for catalytic reaction. Therefore, less steric hindrance and more loadings enhanced the dispersity of the catalysts and the contact area between the reactant and active sites, so that a yield of 93.0 and 46.6 % of ME were obtained from g-p[VDoIm][OH]/MCFs and co-p[VDoIm][OH]/MCFs catalysts respectively.

Figure 8 showed the effect of alkyl side chain of IL on the catalytic performance of PILs/MCFs catalysts. As shown in Fig. 8a, the alkyl side chain had little effect on

Table 2 Element analysis of co-p[VDoIm][OH]/MCFs and g-p[VDoIm][OH]/MCFs

Samples	N element content (wt.%)	Loading amount (c/mmol/g)
co-p[VDoIm][OH]/MCFs	2.4674	0.8809
g-p[VDoIm][OH]/MCFs	3.4057	1.2162

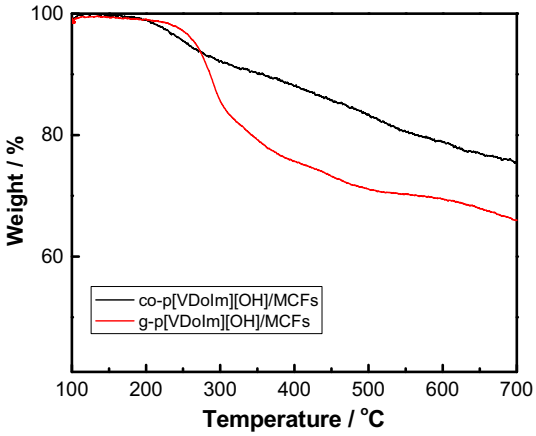

Fig. 5 TG curves of co-p[VDoIm][OH]/MCFs and g-p[VDoIm][OH]/MCFs

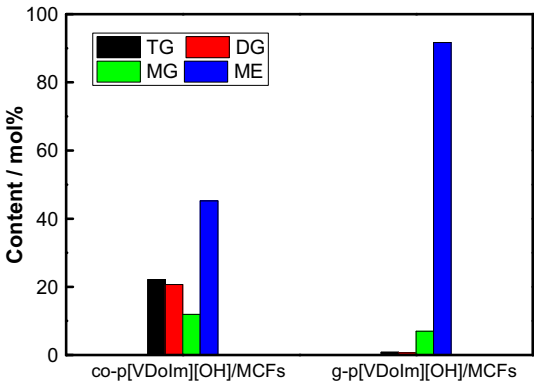

Fig. 6 The catalytic performances of co-p[VDoIm][OH]/MCFs and g-p[VDoIm][OH]/MCFs

the catalytic performance of the co-p[VRIm][OH]/MCFs due to its surface structure. However, the catalytic activity increased rapidly when the alkyl chain increased from C_3 to C_{12} for g-p[VRIm][OH]/MCFs as shown in Fig. 8b. It can be deduced that lauryl group has a better surface activity than propyl and hexyl, which played the role of a surfactant and dispersed the catalysts in the solution effectively, therefore g-p[VDoIm][OH]/MCFs catalysts presented the highest catalytic activity.

The recycling use of the supported poly(IL)s catalysts was investigated, as shown in Fig. 9. It can be seen that the catalytic activities went down in the four cycles for both of PILs/MCFs catalysts. This might be due to the rupture of Si–O–Si chemical bond and the loss of PILs on the surface of MCFs. However, the g-p[VDoIm][OH]/MCFs catalysts still showed a catalytic performance >76.1 % even after four recycling, which indicated that the catalysts had excellent recycle stability.

3.2.2 *Catalytic Performance for Knoevenagel Condensation*

Since lauryl group has better surface dispersion in the catalytic processes than propyl and hexyl, co-p[VDoIm][OH]/MCFs and g-p[VDoIm][OH]/MCFs can be used to evaluate the catalytic performance for the Knoevenagel condensation below.

Figure 10 showed the catalytic performances of PILs/MCFs catalysts for the Knoevenagel condensation. Due to the influence of steric hindrance and active sites, g-p[VDoIm][OH]/MCFs presented a higher catalytic

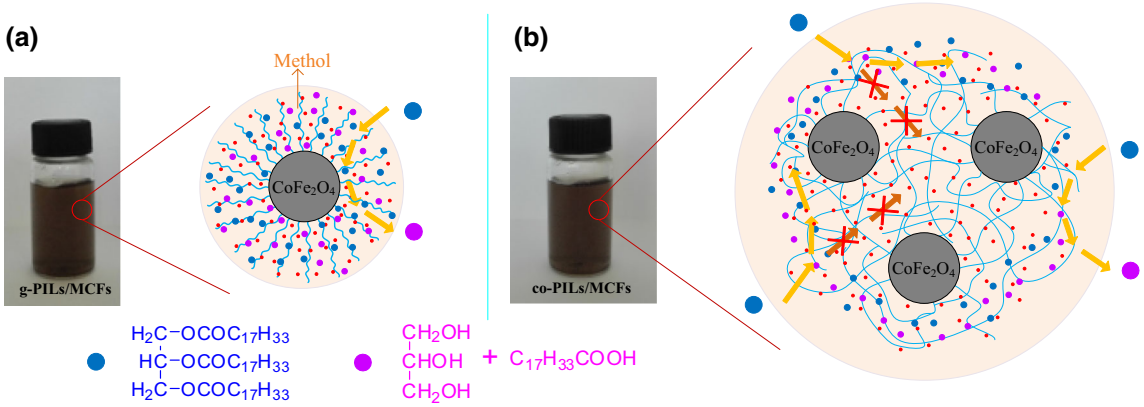

Fig. 7 Catalytic mechanism of **a** g-p[VDoIm][OH]/MCFs and **b** co-p[VDoIm][OH]/MCFs

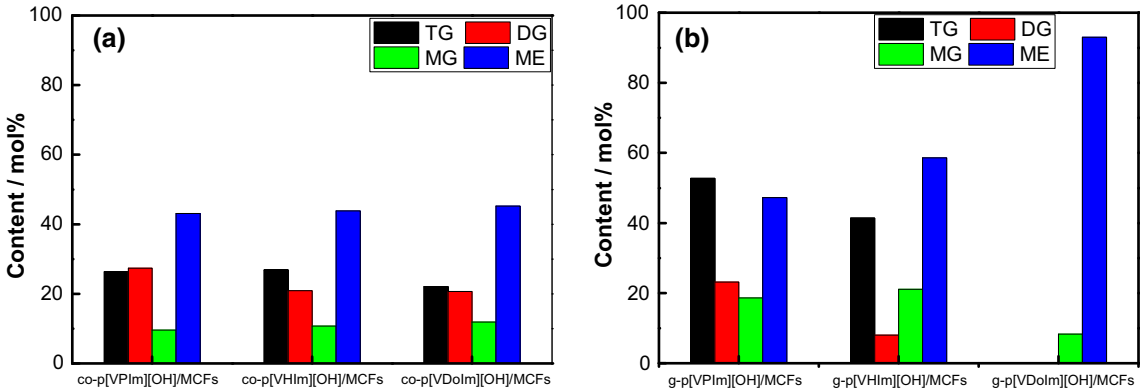

Fig. 8 The catalytic performance of **a** co-p[VRIm][OH]/MCFs, **b** g-p[VRIm][OH]/MCFs

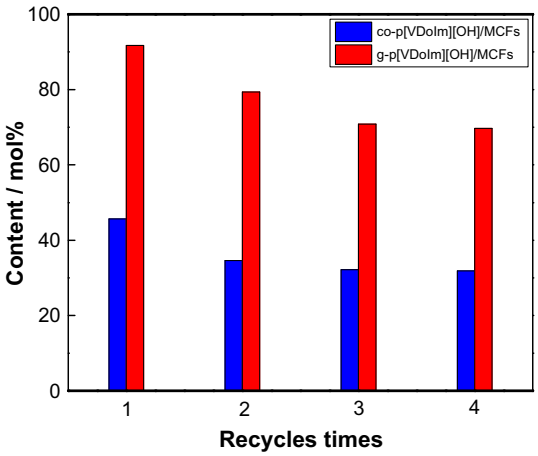

Fig. 9 Recycling of the co-p[VDoIm][OH]/MCFs and g-p[VDoIm][OH]/MCFs catalysts

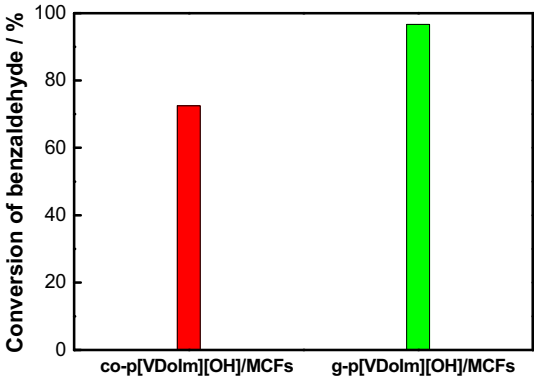

Fig. 10 The catalytic performance of co-p[VDoIm][OH]/MCFs and g-p[VDoIm][OH]/MCFs caltalysts

activity than co-p[VDoIm][OH]/MCFs. The conversion of benzaldehyde was around 97 % for g-p[VDoIm][OH]/MCFs higher than 72.5 % for co-p[VDoIm][OH]/MCFs, which was consistent with the transesterification reaction.

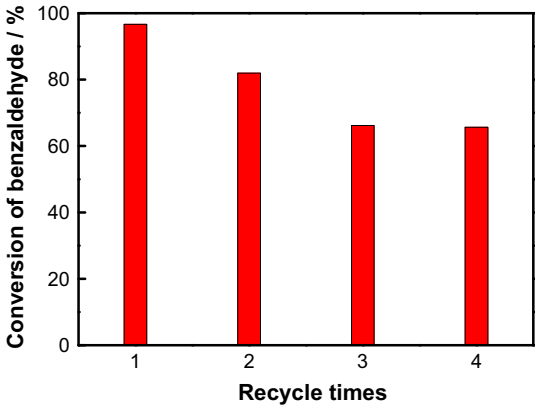

Fig. 11 Recycling of g-p[VDoIm][OH]/MCFs catalyst

However, the activities of both two types of catalysts for Knoevenagel condensation were higher than that for transesterification reaction. This most probably is because the molecular size of benzaldehyde is less than the size of TG, so that benzaldehyde is easier to diffusion into the catalyst inside. The recycling use of the supported g-p[VDoIm][OH]/MCFs catalysts were carried out and the results showed that the catalysts can be recycled four times and maintain a high catalytic activity of around 68.5 %. This means that the catalysts have excellent recycling stability (shown in Fig. 11).

4 Conclusions

MCF grafted basic poly(IL)s catalysts were synthesized through two different methods and their performances were evaluated by the transesterification of TG with methanol and the Knoevenagel condensation of benzaldehyde with ethyl cyanoacetate, respectively. According to a systematic comparison, the g-p[VDoIm][OH]/MCFs catalysts were found to have higher loading amount, better stability and

excellent paramagnetism, and thus higher catalytic efficiency as compared to co-p[VDoIm][OH]/MCFs. The significant enhancement of catalytic activity could be attributed to the cooperativity between active site and steric hindrance. The yields for g-p[VDoIm][OH]/MCFs catalyzing transesterification and Knoevenagel condensation were 93 and 97 %, respectively, and the catalysts could be easily recovered with the assistance of an external magnetic field. Besides, increasing the length of alkyl side chain of IL resulted in a positive trend for catalytic performance. However, the catalytic performance of PILs/MCFs catalysts decreased after being reused four times. Nonetheless, the catalytic performances of g-PILs/MCFs were still above 76.1 % for transesterification and 68.5 % for Knoevenagel condensation respectively after being used for four times, indicating the excellent recycle stability of the supported catalysts.

Acknowledgments We acknowledge the financial support by the National Natural Science Foundation of China (No. 21576025).

References

1. Kresse G, Hafner J (1993) Phys Rev B 47:558
2. Picquet M, Poinsot D, Stutzmann S, Tkatchenko I, Tommasi I, Wasserscheid P, Zimmermann J (2004) Top Catal 29:139
3. Olivier-Bourbigou H, Magna L, Morvan D (2010) Appl Catal A Gen 373:1
4. Jiang CH, Wang HY, Qi L, Gao GT (2013) Chem J Chin Univ 34:231
5. Yuan JY, Mecerreyes D, Antonietti M (2013) Prog Polym Sci 38:1009
6. Mecerreyes D (2011) Prog Polym Sci 36:1629
7. Yuan JY, Antonietti M (2011) Polymer 52:1469
8. Alessandro D, Elena G, Claudia B, Jenny GV, Silvia B (2015) J. Mater. Chem. A 3:8508
9. Sugimura R, Qiao K, Tomida D, Kume Y, Yokoyama C (2007) Chem Lett 36:874
10. Huang Q, Wang LL, Zheng BZ, Long Q (2009) Prog Chem 21:1782
11. Liu WD, Wang DF, Duan YJ, Zhang YH, Bian FL (2015) Tetrahedron Lett 56:1784
12. Bao QX, Qiao K, Tomida D, Yokoyama C (2009) Catal Commun 10:1625
13. Sugimura R, Qiao K, Tomida D, Yokoyama C (2007) Catal Commun 8:770
14. Jiang YY, Guo C, Xia HS, Mahmood I, Liu CZ, Liu HZ (2009) J Mol Catal B Enzym 58:103
15. Dadhania HN, Raval DK, Dadhania AN (2015) Catal Sci Technol 5:4806
16. Wu Z, Li Z, Wu G, Wang L, Lu S, Wang L, Wan H, Guan G (2014) Ind Eng Chem Res 53:3040
17. Trujillo-Rodríguez MJ, Yu HL, Cole WTS, Ho TD, Pino V, Anderson JL, Afonso AM (2014) Talanta 121:153
18. Bi WT, Wang M, Yang XD, Row KH (2014) J Sep Sci 37:1632
19. Pourjavadi A, Hosseini SH, Doulabi Mahmoud Fakoorpoor MS, Seidi F (2012) ACS Catal 2:1259
20. Pourjavadi A, Hosseini SH, Moghaddam FM, Foroushani BK, Bennett C (2013) Green Chem 15:2913
21. Pourjavadi A, Hosseini SH, Aghayee Meibody SA, Hosseini ST (2013) C R Chim 16:906
22. Leng Y, Zhao JW, Jiang PP, Wang J (2014) ACS Appl Mater Interfaces 6:5947
23. Taber A, Kirn JB, Jung JY, Ahn WS, Jin MJ (2009) Synlett 15:2477
24. Zhang YP, Jiao QZ, Zhen B, Wu Q, Li HS (2013) Appl Catal A Gen 453:327
25. Li HS, Zhang YP, Wang SY, Wu Q, Liu CH (2009) J Hazard Mater 169:1045
26. De Palma R, Peeters S, Van Bael MJ, Den Rul HV, Bonroy K, Laureyn W, Mullens J, Borghs G, Maes G (2007) Chem Mater 19:1821
27. Suarez PAZ, Dullius JEL, Einloft S, DeSouza RF, Dupont J (1996) Polyhedron 15:1217
28. Li XQ, Guan P, Hu XL, Tang YM, Lin XP (2013) CIESC J 64:4153
29. Chen XW, Song HB, Chen P, Wang FR, Qian Y, Li XH (2012) Acta Chim Sin 6:770–774